Turkish Journal of Physics

Volume 48 | Number 3 Article 5

2024

Mechanical calculations on atomically thin membranes

BURAK ASLAN

TÜBİTAK

Turkish Journal of Physics

http://journals.tubitak.gov.tr/physics/

Research Article

Turk J Phys
(2024) 48: 115 – 124

doi:10.55730/1300-0101.2761

Mechanical calculations on atomically thin membranes

Burak ASLAN*
Department of Physics, Boğaziçi University, İstanbul, Turkiye

Received: 10.01.2024 • **Accepted/Published Online:** 04.06.2024 • **Final Version:** 13.06.2024

Abstract: We present mechanical calculations on suspended ultrathin membranes on circular holes. Our focus is group-6 transition metal dichalcogenides. We provide computations on strain, stress, deflection, surface area, volume, radius of curvature, gradient, and resonance frequency of membranes. We also provide code in the Python programming language so anyone can repeat these calculations on their material of interest.

Key words: two-dimensional materials, mechanical calculations, suspended membranes, Python

1. Introduction

Numerous studies and reviews have been conducted on the mechanics of atomically thin or so-called two-dimensional (2D) membranes [1–7]. Efforts to obtain suspended 2D materials enabled experiments that revealed their fundamental properties [8–15]. Researchers also demonstrated that 2D materials exhibit drastically different characteristics when suspended. They reported that properties such as thermal conductivity [16, 17], electron mobility [18], chemical effect of the substrate [19], exciton binding energy, and optical dielectric function [20] change significantly if the 2D material is suspended. Achieving strain on suspended 2D materials and studying their mechanical properties has been one of the main branches under scope. In this work, we present a tool to perform mechanical computations on suspended 2D membranes. We provide a code in the Python programming language that can calculate the mechanical properties of 2D membranes, such as strain, stress, deflection, surface area, volume, radius of curvature, gradient, and resonance frequency.

2. Mechanical properties of the materials

We list the mechanical properties of MoS_2, $MoSe_2$, $MoTe_2$, WS_2, WSe_2, graphene, aluminum, and gold in Table 1 below. We limit the listing to the parameters needed for the calculations mentioned in this study. The properties of aluminum and gold belong to the bulk thickness, and they may need to be adjusted for the thicknesses of the membranes studied. Many publications on the mechanical properties of the 2D materials listed in Table 1 are available in the literature, but we only mention those that report results on all [21]. Thicknesses of the graphene and other 2D materials are from Ref. [22, 23]. We cite the typical values of breaking strain and strength of MoS_2 available in the literature so that the maximum pressure the membrane can sustain can be calculated [24, 25].

*Correspondence: aslan@bogazici.edu.tr

Table 1. Mechanical properties of the materials of interest.

Material	Thickness (nm)	$E_{2D} = E_{3D}t$ (N/m)	E_{3D} (GPa)	Breaking strength (GPa)	Breaking strain (%)	Poisson's ratio	Mass density (g/cm^3)
MoS_2	0.615 [23]	124.5 [21]	202.4 [21]	16-30 [25]	6-11 [25]	0.25 [21]	5.06
$MoSe_2$	0.646 [23]	103.9 [21]	160.8 [21]			0.23 [21]	6.9
$MoTe_2$	0.698 [23]	79.4 [21]	113.8 [21]			0.24 [21]	7.7
WS_2	0.618 [23]	139.6 [21]	225.9 [21]			0.22 [21]	7.5
WSe_2	0.649 [23]	116.0 [21]	178.7 [21]			0.19 [21]	9.32
Graphene	0.335 [22]	341.0 [21]	1017.9 [21]			0.18 [21]	2.27
Aluminum	Bulk		68.0			0.36	2.71
Gold	Bulk		77.2			0.42	19.3

Even though we focus on atomically thin materials in this study, we will also inspect ultrathin folio of metals such as aluminum and gold that have been commercially available. Large-size aluminum folios as thin as 7.5 nm and gold folios as thin as 1 µm are available in the market. Researchers demonstrated thinner gold folios that may not be available commercially. As such metals are stable, sturdy, and have high conductivity and close to 1 optical reflectance, using them as suspended membranes might be preferable over using 2D materials for specific applications. We present some calculations on metal membranes as well.

3. Structure and Hencky's solution

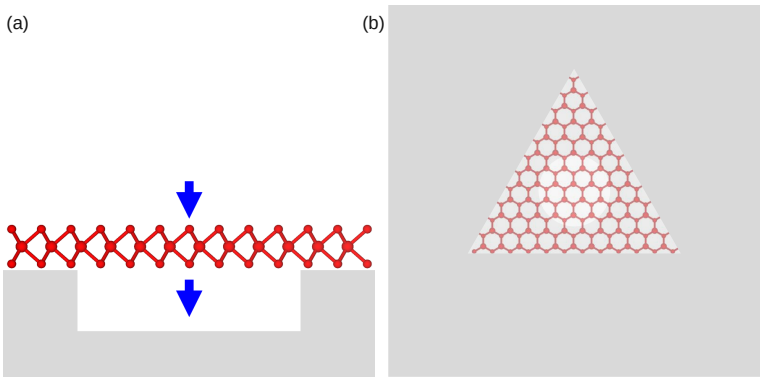

Figure 1. Schematic of a membrane on a circular hole ((a) side view, (b) top view). Blue arrows indicate the direction of the deflection under external air pressure.

We inspect the behavior of a uniform membrane placed on a circular hole under uniform air pressure. Figure 1 depicts the schematic of the structure. We assume the membrane does not slide on or delaminate from the surface (clamped at the hole edge). For the simplicity of the calculations, we assume uniform lateral loading (so-called Hencky's problem) instead of uniform pressure for the calculations. The uniform loading model neglects the radial pressure component on the deflected

membrane. We will review the validity of that assumption afterward. The biaxial strain, ϵ, vertical deflection, h, radial and tangential stress, N_r and N_θ at the center of a uniformly loaded circular membrane clamped at radius a are given by [26]:

$$\begin{aligned}
\epsilon(r=0) &= \frac{(1-\nu)\,b_0}{4}\left(\frac{Pa}{E_{3D}t}\right)^{\frac{2}{3}}, \\
h(r=0) &= \frac{a}{b_0}\left(\frac{Pa}{E_{3D}t}\right)^{\frac{1}{3}}, \\
N_r(r=0) = N_\theta(r=0) &= \frac{b_0}{4}E_{3D}t\left(\frac{Pa}{E_{3D}t}\right)^{\frac{2}{3}}, \\
\epsilon(r=0) &= \frac{(1-\nu)\,b_0^3}{4}\left(\frac{h}{a}\right)^2
\end{aligned} \tag{1}$$

Here P is the air pressure difference between the two sides of the membrane (which we refer to as "pressure" in this work), ν is Poisson's ratio of the membrane, b_0 is a parameter dependent on ν, E_{3D} is the 3D Young's modulus (modulus of elasticity), t is the membrane thickness, r is the radial distance from the center. The quantity $E_{3D}t$ is also called the 2D elastic modulus, E_{2D}. We assume all these material properties remain invariant as the sample deflects and stretches. We also assume that there is no pre-tension on the membrane; when the pressure is zero, the tension is also zero. We compute the strain, ϵ, vertical deflection, h, radial and tangential stress, N_r and N_θ for $0 \le r \le a$ by using equations (3, 4, 12, 20-31, 34) in Ref. [26]. We show the calculated deflection, strain, and stress at the center of a 1L WS_2 membrane as a function of pressure for various diameter values in Figure 2. It shows that the deflection is very sensitive to slight pressure variations around low-pressure levels as the deflection is proportional to the one-third power of pressure. However, strain and stress are proportional to the two-thirds power of pressure, and they are less sensitive to pressure for low-pressure levels. Deflection is proportional to the four-third power of the radius, and the above effect is more apparent for larger radius values.

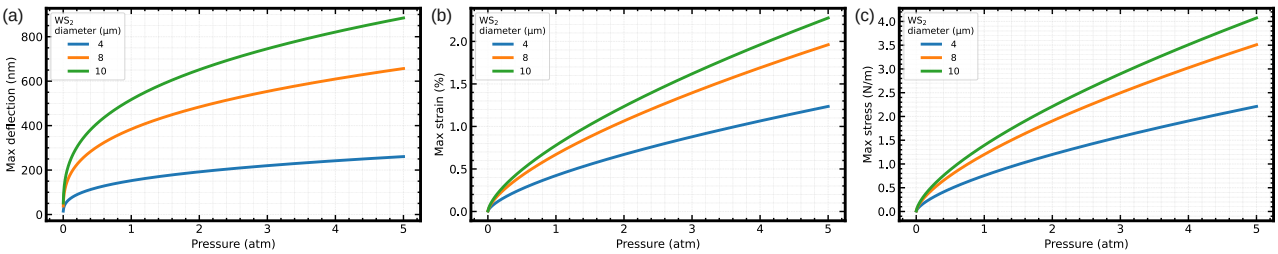

Figure 2. (a) Deflection, (b) strain, and (c) stress at the center of the membrane as a function of pressure (material is 1L WS_2).

To examine the distribution of the strain, vertical deflection, and radial and tangential stress on the membrane, we compute them for $0 \le r \le a$ by using equations (3, 4, 12, 20-31, 34) in Ref. [26]. Figure 3 shows the calculations on a 1L WS_2 with a diameter of 12 μm at various pressure values. It is worth noting that the radial strain slowly decreases away from the center, whereas the tangential strain is zero at the edges of the membrane due to the boundary condition.

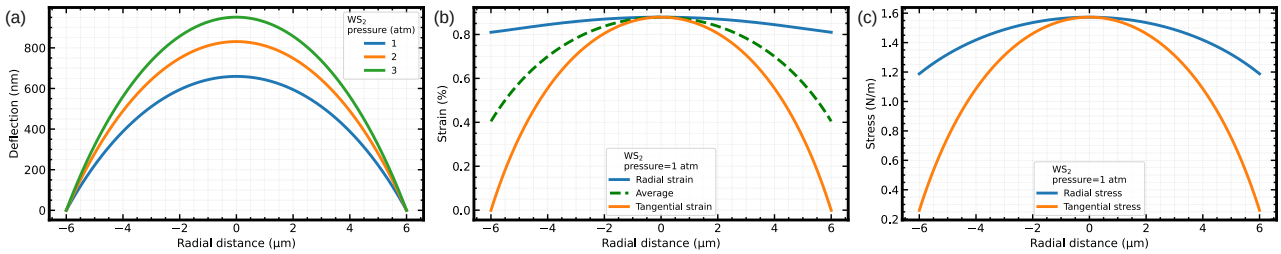

Figure 3. (a) Deflection, (b) strain, and (c) stress as a function of radial distance on the membrane (material is 1L WS_2).

Once the deflection of the membrane is calculated everywhere on the membrane, we can calculate the radius of curvature, surface area, volume, and gradient. We refer to the volume between the flat and deflected membrane as the volume of the membrane, V. It can be calculated as the sum of the volume of the infinitely small cylindrical shells with radius r, thickness dr, and height $h(r)$. The area of the membrane, A, can be calculated as the sum of the area of the infinitely small rings. They are given in the equation below:

$$V = \int_0^a 2\pi r h(r)\, dr,$$
$$A = \int_0^a \frac{2\pi r}{\cos(\theta(r))} dr = \int_0^a \frac{2\pi r}{\sqrt{1+\tan^2(\theta(r))}} dr = \int_0^a \frac{2\pi r}{\sqrt{1+\left(\frac{dh}{dr}\right)^2}} dr, \tag{2}$$

We compare the volume and area of the membrane given in eq. (2) to that of a paraboloid ($V_{paraboloid} = \frac{1}{2}\pi h a^2, A_{paraboloid} = \frac{\pi a^4}{6h^2}\left[\left(1+4\left(\frac{h}{a}\right)^2\right)^{\frac{3}{2}} - 1\right]$) with the same height and radius in Figure 4. The relative deviation of the membrane's area from the paraboloid's area is minimal, even for high-pressure values. Both of the area values reduce to πa^2 for small deflection. The same deviation is large in the case of the volumes. Interestingly, the volume deviation is independent of pressure. The volume deviation depends on the material but not the radius. Volume and deflection have a similar dependence on pressure, as expected. The paraboloid approximation underestimates the membrane's area and volume in all cases.

We calculate the angle between the tangential in the outward direction and the horizontal, $\theta(r)$, the focal length as a function pressure as $F(r) = \frac{R(r)}{2}$ from the radius of curvature, $R(r)$, and for comparison, the focal length of a paraboloid with the same maximum deflection as the membrane at its center $F_{paraboloid}(r=0)$ as follows:

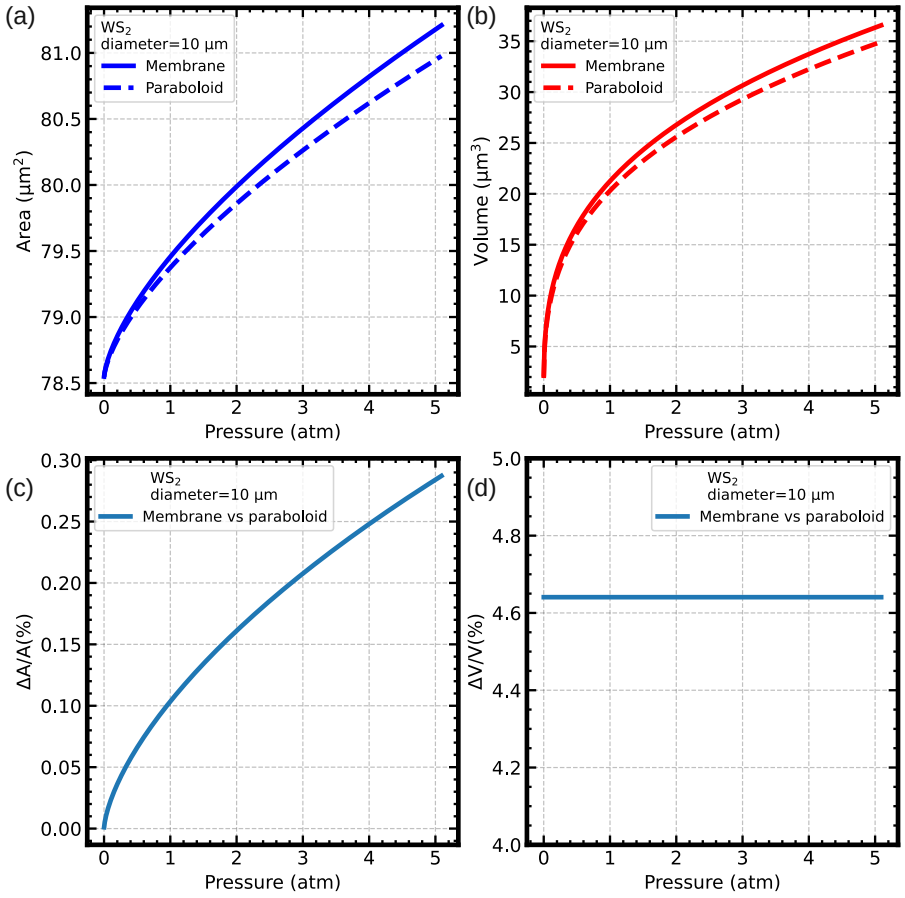

Figure 4. Comparison of calculated volumes and areas of a monolayer WS_2 membrane under air pressure and a paraboloid shape with the same height as the maximum deflection of the membrane.

$$\theta(r) = \tan^{-1}\left(\frac{dh}{dr}\right),$$

$$F(r) = \frac{\left(1 + \left(\frac{dh}{dr}\right)^2\right)^{\frac{3}{2}}}{2\left|\frac{d^2h}{dr^2}\right|}, \tag{3}$$

$$F_{paraboloid}(r=0) = \frac{a^2}{4h(r=0)} = a\frac{b_0}{4}\left(\frac{E_{3D}t}{Pa}\right)^{\frac{1}{3}}$$

Figure 5 shows the calculations mentioned above on a membrane with a diameter of 12 μm. The angle at the hole's edge goes well above 10 degrees, making it nonnegligible, even at a pressure of 1 atm. $R(r)$ varies relatively little around the center. The focal length at the center is on the order of the hole's radius and decreases with the third power of pressure. The focal length values at the centers of the parabola and membrane are close to each other for large pressure values. However, the membrane's shape deviates from a parabola, and the focal lengths of the two differ more away from

the center.

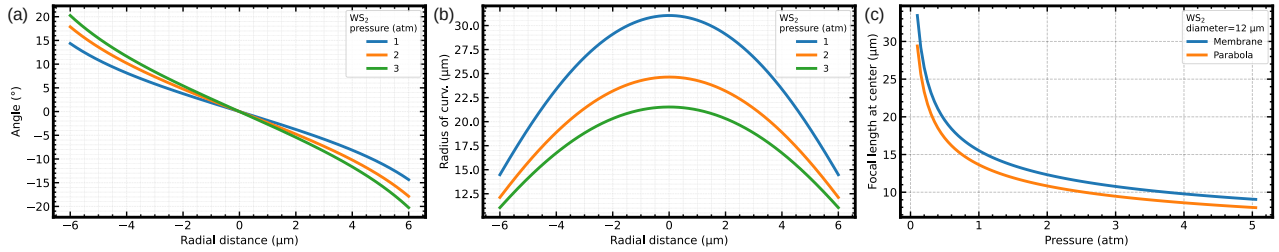

Figure 5. (a) The angle between the tangential to the membrane in the radial and horizontal directions, (b) the radius of curvature of the membrane in the radial direction for various pressure levels, (c) focal length at the center of the membrane and parabola as a function of pressure (material is 1L WS_2).

For the validity of assuming uniform loading instead of uniform pressure, the loading parameter $Pa/E_{3D}t$ should be less than 0.1, as Fichter reported. In our calculations, it is around 0.015 for P = 5 atm and a = 4 μm on a typical monolayer membrane. Thus, that assumption is valid for the calculations in this study, and we use the uniform loading model instead of the more complicated uniform pressure model. However, as Fichter stated, the uniform-pressure loading causes a more nearly spherical shape that is even farther away from the ideal paraboloid than the shape predicted by the solution to Hencky's problem [26].

4. Resonance frequency of 2D membranes

We discuss the resonance frequency of suspended ultrathin membranes. We consider a circular membrane placed on a hole and clamped at the edges of the hole. The structure will possess membrane-like and plate-like vibrations. For a membrane-like and a plate-like circular resonator, the resonance frequencies are given by [27, 28]:

$$f_{m,n}^{membrane} = \frac{j_{m,n}c}{2\pi a},$$
$$f_{m,n}^{plate} = \frac{(\gamma_{m,n}a)^2}{2\pi a^2\sqrt{12(1-\nu^2)}}c_B t, \tag{4}$$

where $j_{m,n}$ are the zero crossings of the Bessel functions with $J_m(x_n)$=0, a is the radius, $c = \sqrt{\frac{T}{\rho t}}$ is the speed of transverse waves, T is the initial pre-tension (in N/m), ρ is the mass density, and t is the thickness. The fundamental frequency of a membrane-like resonator is $f_{0,1}^{membrane} = \frac{2.4048c}{2\pi a}$.

$\gamma_{m,n}a$ gives the resonance frequencies of plate-like resonators with the fundamental value of $\gamma_{0,1}a$=3.19622, and $c_B = \sqrt{\frac{E_{3D}}{\rho}}$ is the longitudinal wave speed in bars. The fundamental frequency of a plate-like resonator is $f_{0,1}^{plate} = \frac{10.2158}{2\pi a^2\sqrt{12(1-\nu^2)}}c_B t$. As stated by Garrett, the vibration of thin plates has the same relationship to the vibration of membranes as the flexural vibration of bars has to the transverse vibrations of a limp string [28]. The resonance frequency of the mechanical resonators in the cross-over regime of plate to membrane can be calculated as $f \cong \sqrt{f^{plate^2} + f^{membrane^2}}$ [14].

Figure 6a shows the lowest resonant frequency of a circular 1L WS_2 membrane as a function of the membrane diameter. Figure 6b shows the lowest resonant frequency of a 2 µm diameter circular WS_2 membrane for various thicknesses. We take the pre-tension in the WS_2 membranes as 0.02 N/m [6, 13].

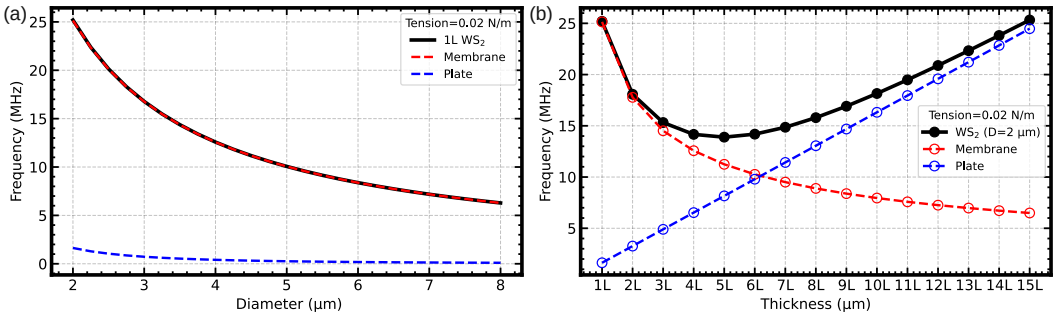

Figure 6. (a) The fundamental frequency of a circular 1L WS_2 membrane as a function of diameter, (b) the fundamental frequency of a 2 µm diameter circular WS_2 membrane for various thicknesses. In both cases, the pre-tension in the membrane is 0.02 N/m. Membrane and plate-like vibrational frequencies are in red and blue, respectively.

As a comparison, we repeat the calculations above on an aluminum membrane about 1500 times greater in dimensions. Figure 7a shows the lowest resonant frequency of a circular 1 µm thick aluminum membrane as a function of diameter. Figure 7b shows the lowest resonant frequency of a 3000 µm diameter circular aluminum membrane for various thicknesses. To determine a reasonable pre-tension on the aluminum membrane, we calculate the stress on a 2 µm diameter circular 1L WS_2 membrane and find that a pressure of around 0.015 atm causes an average stress of about 0.02 N/m. The same pressure causes an average stress of about 20 N/m on the 3000 µm diameter and 1 µm thick aluminum membrane. In both cases shown in Figure 7, the pre-tension in the aluminum membranes is 20 N/m.

In both materials, the frequency is dominated by the membrane-like vibrations at small thicknesses, but plate-like vibrations become more dominant with increasing thickness. The resonant frequencies of both components decrease with increasing diameter.

5. Codes for calculations

The model used for the calculations in this study has been used in several studies and yielded material properties that agree with the experimental results [11, 12, 14, 20, 29–31]. As the model has been so helpful for studies on 2D materials, a simple tool ready to use will benefit the scientific community. We are including the link to the codes we used to perform the calculations given as supplemental material in this publication (see "Data availability" section at the end). Our codes can be modified to repeat the calculations on other materials or for different dimensions or parameters.

6. Conclusions

We have performed mechanical calculations on uniform suspended ultrathin membranes on circular holes. We have reported strain, stress, deflection, surface area, volume, radius of curvature, gradient, and resonance frequency calculations in suspended ultrathin membranes. Applications relying on thin

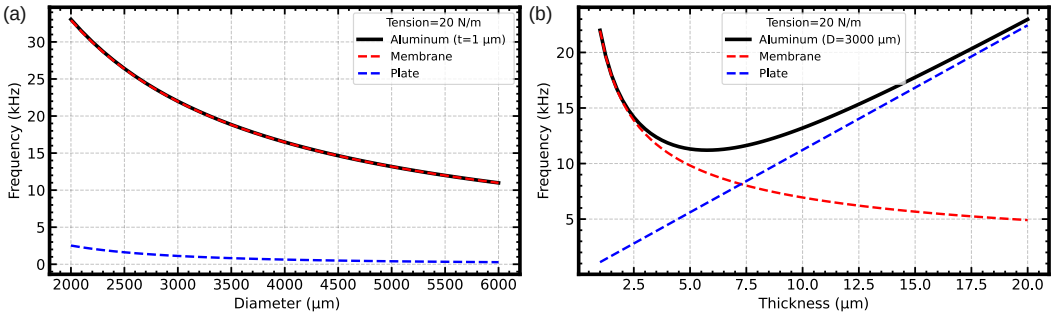

Figure 7. (a) The fundamental frequency of a circular 1 μm thick aluminum membrane as a function of diameter, (b) the fundamental frequency of a 3000 μm diameter circular aluminum membrane for various thicknesses. In both cases, the pre-tension in the membrane is 20 N/m. Membrane and plate-like vibrational frequencies are in red and blue, respectively.

membranes, such as fiber-optic sensors, can benefit from the calculation capabilities we present here [32, 33]. Applying air pressure to two-dimensional materials is one of the most common techniques, and we hope our results will be helpful in expanding universe of research on 2D materials.

Data availability

The data supporting this study's findings are available from the corresponding author upon reasonable request. The codes we provide can also reproduce the data and can be accessed via the following link: https://aperta.ulakbim.gov.tr/record/273702.

Conflict of interest

The author has no conflicts to disclose.

Acknowledgments

We acknowledge the support by Boğaziçi University Scientific Research Projects (Project number 21B03SUP4) and TÜBİTAK (The Scientific and Technological Research Council of Türkiye) (Project number 118C325). TÜBİTAK's support does not imply any endorsement of the scientific content of this work.

References

[1] Z. Lin, Y. Lei, S. Subramanian, N. Briggs, Y. Wang et al., "Research Update: Recent progress on 2D materials beyond graphene: From ripples, defects, intercalation, and valley dynamics to straintronics and power dissipation," *APL Mater.* **6** (2018) 80701.

[2] D. Akinwande, C. J. Brennan, J. S. Bunch, P. Egberts, J. R. Felts et al., "A review on mechanics and mechanical properties of 2D materials—Graphene and beyond," *Extrem. Mech. Lett.* **13** (2017) 42–77.

[3] G. G. Naumis, S. Barraza-Lopez, M. Oliva-Leyva, and H. Terrones, "Electronic and optical properties of strained graphene and other strained 2D materials: a review," *Reports Prog. Phys.* **80** (2017) 096501.

[4] C. Di Giorgio, E. Blundo, G. Pettinari, M. Felici, F. Bobba et al., "Mechanical, Elastic, and Adhesive Properties of Two-Dimensional Materials: From Straining Techniques to State-of-the-Art Local Probe Measurements," *Adv. Mater. Interfaces* **9** (2022) 2102220.

[5] C. Androulidakis, K. Zhang, M. Robertson, and S. Tawfick, "Tailoring the mechanical properties of 2D materials and heterostructures," *2D Mater.* **5** (2018) 032005.

[6] A. Castellanos-Gomez, V. Singh, H. S. J. van der Zant, and G. A. Steele, "Mechanics of freely-suspended ultrathin layered materials," *Ann. Phys.* **527** (2015) 27–44.

[7] J. H. Kim, J. H. Jeong, N. Kim, R. Joshi, and G.-H. Lee, "Mechanical properties of two-dimensional materials and their applications," *J. Phys. D. Appl. Phys.* **52** (2019) 083001.

[8] I. W. Frank, D. M. Tanenbaum, A. M. van der Zande, and P. L. McEuen, "Mechanical properties of suspended graphene sheets," *J. Vac. Sci. Technol. B Microelectron. Nanom. Struct. Process. Meas. Phenom.* **25** (2007) 2558–2561.

[9] C. Lee, X. Wei, J. W. Kysar, and J. Hone, "Measurement of the Elastic Properties and Intrinsic Strength of Monolayer Graphene," *Science* **321** (2008) 385–388.

[10] R. Zhang, V. Koutsos, and R. Cheung, "Elastic properties of suspended multilayer WSe2," *Appl. Phys. Lett.* **108** (2016) 042104.

[11] D. Lloyd, X. H. Liu, J. W. Christopher, L. Cantley, A. Wadehra et al., "Band Gap Engineering with Ultralarge Biaxial Strains in Suspended Monolayer MoS2," *Nano Lett.* **16** (2016) 5836–5841.

[12] J. S. Bunch, S. S. Verbridge, J. S. Alden, A. M. van der Zande, J. M. Parpia et al., "Impermeable atomic membranes from graphene sheets," *Nano Lett.* **8** (2008) 2458–2462.

[13] A. Castellanos-Gomez, M. Poot, G. A. Steele, H. S. J. van der Zant, N. Agraït et al., "Elastic Properties of Freely Suspended MoS2 Nanosheets," *Adv. Mater.* **24** (2012) 772–775.

[14] A. Castellanos-Gomez, R. van Leeuwen, M. Buscema, H. S. J. van der Zant, G. A. Steele et al., "Single-Layer MoS2 Mechanical Resonators," *Adv. Mater.* **25** (2013) 6719–6723.

[15] A. L. Kitt, Z. Qi, S. Rémi, H. S. Park, A. K. Swan et al., "How Graphene Slides: Measurement and Theory of Strain-Dependent Frictional Forces between Graphene and SiO2," *Nano Lett.* **13** (2013) 2605–2610.

[16] S. Chen, Q. Wu, C. Mishra, J. Kang, H. Zhang et al., "Thermal conductivity of isotopically modified graphene," *Nat. Mater.* **11** (2012) 203–207.

[17] A. A. Balandin, S. Ghosh, W. Bao, I. Calizo, D. Teweldebrhan et al., "Superior Thermal Conductivity of Single-Layer Graphene," *Nano Lett.* **8** (2008) 902–907.

[18] K. I. Bolotin, K. J. Sikes, Z. Jiang, M. Klima, G. Fudenberg et al., "Ultrahigh electron mobility in suspended graphene," *Solid State Commun.* **146** (2008) 351–355.

[19] F. Sarcan, A. J. Armstrong, Y. K. Bostan, E. Kus, K. P. McKenna et al., "Ultraviolet-Ozone Treatment: An Effective Method for Fine-Tuning Optical and Electrical Properties of Suspended and Substrate-Supported MoS2," *Nanomaterials* **13** (2023) 3034.

[20] B. Aslan, C. Yule, Y. Yu, Y. J. Lee, T. F. Heinz et al., "Excitons in strained and suspended monolayer WSe2," *2D Mater.* **9** (2022) 015002.

[21] D. Çakır, F. M. Peeters, and C. Sevik, "Mechanical and thermal properties of h -MX2 (M = Cr, Mo, W; X = O, S, Se, Te) monolayers: A comparative study," *Appl. Phys. Lett.* **104** (2014) 203110.

[22] R. E. Franklin, "The structure of graphitic carbons," *Acta Crystallogr.* **4** (1951) 253–261.

[23] J. A. Wilson and A. D. Yoffe, "The transition metal dichalcogenides discussion and interpretation of the observed optical, electrical and structural properties," *Adv. Phys.* **18** (1969) 193–335.

[24] G. Wang, Y. Wang, S. Li, Q. Yang, D. Li et al., "Engineering the Crack Structure and Fracture Behavior in Monolayer MoS 2 By Selective Creation of Point Defects," *Adv. Sci.* **9** (2022) 2200700.

[25] S. Bertolazzi, J. Brivio, and A. Kis, "Stretching and Breaking of Ultrathin MoS2," *ACS Nano* **5** (2011) 9703–9709.

[26] W. B. Fichter, "Some Solutions for the Large Deflections of Uniformly Loaded Circular Membranes," *NASA Technol. Pap.* **3658** (1997) 1–24.

[27] T. Wah, "Vibration of Circular Plates," *J. Acoust. Soc. Am.* **34** (1962) 275–281.

[28] S. L. Garrett, "Understanding Acoustics," *Cham, Switzerland: Springer International Publishing* (2020).

[29] J. J. Vlassak and W. D. Nix, "A new bulge test technique for the determination of Young's modulus and Poisson's ratio of thin films," *J. Mater. Res.* **7** (1992) 3242–3249.

[30] D. Metten, F. Federspiel, M. Romeo, and S. Berciaud, "All-Optical Blister Test of Suspended Graphene Using Micro-Raman Spectroscopy," *Phys. Rev. Appl.* **2** (2014) 054008.

[31] G. Wang, Z. Dai, Y. Wang, P. Tan, L. Liu et al., "Measuring Interlayer Shear Stress in Bilayer Graphene," *Phys. Rev. Lett.* **119** (2017) 036101.

[32] Z. Liu, H. Cao, and F. Xu, "Fiber-optic Lorentz force magnetometer based on a gold-graphene composite membrane," *Appl. Phys. Lett.* **112** (2018).

[33] B. Zheng, S. Yan, J. Chen, G. Cui, F. Xu et al., "Miniature optical fiber current sensor based on a graphene membrane," *Laser Photon. Rev.* **9** (2015) 517–522.